

# <sup>1</sup> The Morphological Diversification of Siphonophore Tentilla

<sup>3</sup> Alejandro Damian-Serrano<sup>1,‡</sup>, Steven H.D. Haddock<sup>2</sup>, Casey W. Dunn<sup>1</sup>

<sup>4</sup> <sup>1</sup> Yale University, Department of Ecology and Evolutionary Biology, 165 Prospect St.,  
<sup>5</sup> New Haven, CT 06520, USA

<sup>6</sup> <sup>2</sup> Monterey Bay Aquarium Research Institute, 7700 Sandholdt Rd., Moss Landing, CA  
<sup>7</sup> 95039, USA

<sup>8</sup> <sup>‡</sup> Corresponding author: Alejandro Damian-Serrano, email: alejandro.damianserrano@  
<sup>9</sup> yale.edu

## <sup>10</sup> Abstract

<sup>11</sup> Siphonophore tentilla (tentacle side branches) are unique biological structures for prey capture,  
<sup>12</sup> composed of a complex arrangement of cnidocytes (stinging cells) bearing different types  
<sup>13</sup> of nematocysts (stinging capsules) and auxiliary structures. Tentilla present an exuberant  
<sup>14</sup> morphological diversity of form and function across species. While associations between  
<sup>15</sup> tentilla form and diet have been reported, the evolutionary history giving rise to this  
<sup>16</sup> morphological diversity is largely unexplored. Here we explore the evolutionary gains and  
<sup>17</sup> losses of novel tentillum substructures and nematocyst types on the most recent siphonophore  
<sup>18</sup> phylogeny. Tentilla have a precisely coordinated high-speed strike mechanism of synchronous  
<sup>19</sup> unwinding and nematocysts discharge. Here we characterize the kinematic diversity of this  
<sup>20</sup> prey capture reaction using high-speed video and find relationships with morphological  
<sup>21</sup> characters. Since tentillum discharge occurs in synchrony across a broad morphological  
<sup>22</sup> diversity, we evaluate how phenotypic integration is maintaining character correlations across  
<sup>23</sup> evolutionary time. Moreover, we analyze the dimensionality of the tentillum morphospace,  
<sup>24</sup> identify instances of heterochrony and morphological convergence, and generate hypotheses  
<sup>25</sup> on the diets of understudied siphonophore species. Our findings indicate that siphonophore

<sup>26</sup> tentilla are phenotypically integrated structures with a complex evolutionary history leading to  
<sup>27</sup> a phylogenetically structured diversity of forms which are predictive of kinematic performance  
<sup>28</sup> and feeding habits.

<sup>29</sup> **Keywords**

<sup>30</sup> Siphonophore, tentilla, nematocysts, character evolution

<sup>31</sup> **Introduction**

<sup>32</sup> Siphonophores have fascinated zoologists for centuries for their extremely subspecialized  
<sup>33</sup> colonial organization and integration. Today we hold more knowledge than ever on the  
<sup>34</sup> morphological diversity of this group due to the extensive work of siphonophore taxonomists  
<sup>35</sup> in the past few decades (cite Phil, Steve, etc), which has been elegantly synthesized in detailed  
<sup>36</sup> synopsis (1). In addition, recent advances in phylogenetic analyses of siphonophores (3, 4)  
<sup>37</sup> have provided a macroevolutionary context to interpret this diversity. With these assets in  
<sup>38</sup> hand, we can now begin to study siphonophores from an orthogonal perspective, focusing on  
<sup>39</sup> the diversity and evolutionary history of specific structures. Here we focus on one of such  
<sup>40</sup> structures: the tentilla. Like many cnidarians, siphonophore tentacles bear side branches  
<sup>41</sup> (tentilla) with nematocysts. But unlike other cnidarians, most siphonophore tentilla are  
<sup>42</sup> dynamic structures that react to prey encounters by shooting the nematocyst battery to slap  
<sup>43</sup> around the prey. This maximizes the surface area of contact between the nematocysts and  
<sup>44</sup> the prey they fire upon. In addition, siphonophore tentilla present a remarkable diversity  
<sup>45</sup> of morphologies, sizes, and nematocyst complements (Fig, /???(figure2)). Our overarching  
<sup>46</sup> aim is to organize all this phenotypic diversity in a phylogenetic context, and identify the  
<sup>47</sup> evolutionary processes that generated it.

<sup>48</sup> In (4), we collected the most extensive morphological dataset on siphonophore tentilla and  
<sup>49</sup> nematocysts using state-of-the-art microscopy techniques, and expanded the taxon sampling  
<sup>50</sup> of the phylogeny to disentangle the evolutionary history. The analyses we carried out led

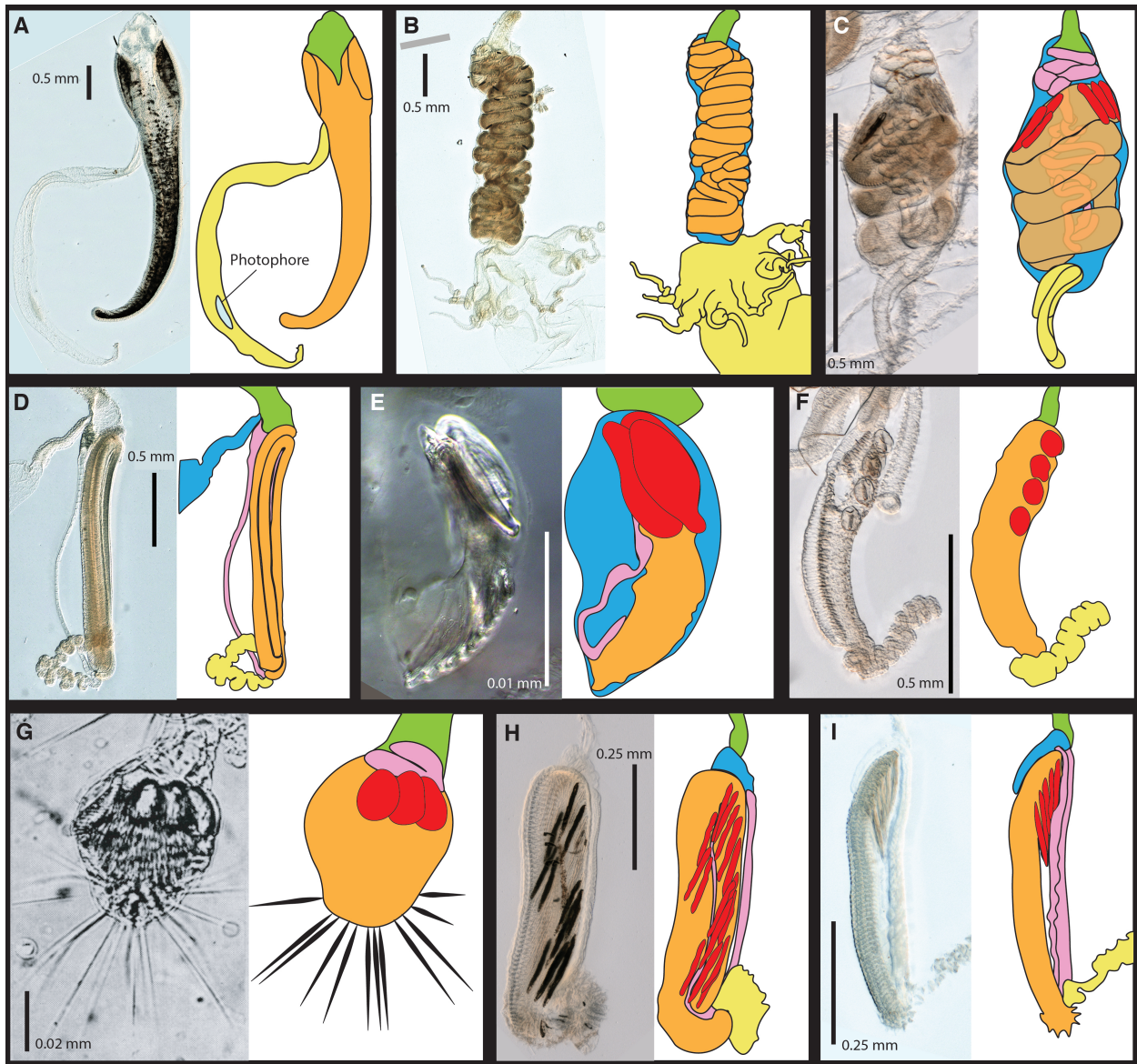


Figure 1: Tentillum diversity. The illustrations delineate the pedicle (green), involucrum (blue), cnidoband (orange), elastic strands (pink), terminal structures (yellow). Heteroneme nematocysts (stenoteles in C,E,F,G and mastigophores in H,I) are depicted in red for some species. A - *Erenna laciniata*, 10x. B - *Lychnagalma utricularia*, 10x. C - *Agalma elegans*, 10x. D - *Resomia ornicephala*, 10x. E - *Frillagalma vityazi*, 20x. F - *Bargmannia amoena*, 10x. G - *Cordagalma* sp., reproduced from Carré 1968. H - *Lilyopsis fluoracantha*, 20x. I - *Abylopsis tetragona*, 20x.

51 to novel, generalizable insights into the evolution of predatory specialization. The work  
52 we present here is complementary to (4), showcasing a far more detailed account on the  
53 evolutionary history of tentilla morphology.

54 Nematocysts are unique biological weapons for defense and prey capture exclusive to  
55 the phylum Cnidaria. Mariscal ((5)) reported that hydrozoans have the largest diversity of  
56 nematocyst types among cnidarians. Among them, siphonophores present the greatest variety  
57 of types (2), and vary widely across taxa in which and how many types they carry on their  
58 tentacles. While recent descriptive studies have expanded and confirmed our understanding  
59 of this diversity, the evolutionary history of nematocyst type gain and loss in siphonophores  
60 remains unexplored. Thus, here we reconstruct the evolution of shifts, gains, and losses of  
61 nematocyst types, subtypes, and other major categorical traits that led to the extant diversity  
62 we see in siphonophore tentilla. In (4), we found strong associations between piscivory  
63 and haploneme shape. These associations could have been produced by convergent changes  
64 in the adaptive optima of these characters. Here we set out to test this hypothesis using  
65 comparative model fitting methods. Analyzing the diversity of morphological states from a  
66 phylogenetic perspective allows us to identify the specific evolutionary processes that gave  
67 rise to it. Here we fit and compare a variety of macroevolutionary models to siphonophore  
68 tentilla morphology measurement data to identify instances of neutral divergence, stabilizing  
69 selection, changes in the speed of evolution, convergent evolution, and paedomorphosis (larval  
70 characters present in mature colonies).

71 In (4) we fitted discriminant analyses to identify characters that are predictive of feeding  
72 guild. These discriminant analyses can be used to generate hypotheses on the diets of  
73 ecologically understudied siphonophore species for which we have morphology data. Here  
74 we present a Bayesian prediction for the feeding guild of 45 species using the morphological  
75 dataset in (4). As mentioned above, tentilla are far from being ornamental shapes and  
76 are in fact violently reactive weapons for prey capture (4, 6). While we now have detailed  
77 characterizations of tentilla morphologies across many species, the diversity of dynamic

78 performances and their relationships to the undischarged morphologies have not been examined  
79 to date. To address this gap, we set out to record high-speed video of the *in vivo* discharge  
80 dynamics of several siphonophore species at sea, and compare the kinematic attributes to  
81 their morphological characters.

## 82 Methods

83 All character data and the phylogeny analyzed here were published in (4). We log transformed  
84 all the continuous characters that did not pass Shapiro-Wilks normality tests, and used the  
85 ultrametric constrained Bayesian time tree in all comparative analyses. When missing data  
86 was incorporated as inapplicable states, we removed those species with characters that could  
87 not be measured due to technical limitations. We used the feeding guild categories detailed  
88 in (4) with one modification: including all *Forskalia* spp. as generalists not only a single  
89 *Forskalia* species on the tree after a reinterpretation of the data in (7). In order to characterize  
90 the evolutionary history of tentilla morphology, we fitted different models generating the  
91 observed data distribution given the phylogeny for each continuous character using the  
92 function fitContinuous in the R package *geiger* (8). These models include a non-phylogenetic  
93 white-noise model (WN), a neutral divergence Brownian Motion model (BM), an early-burst  
94 decreasing rate model (EB), and an Ornstein-Uhlenbeck (OU) model with stabilizing selection  
95 around a fitted optimum trait value. In the same way as (4) we then ordered the models  
96 by increasing parametric complexity (WN, BM, EB, OU), and compared their corrected  
97 Akaike Information Criterion (AICc) scores (9). We used the lowest (best) score using a delta  
98 cutoff of 2 units to determine significance relative to the next simplest model (SM10). We  
99 calculated model adequacy scores using the R package *arbutus* (10) (SM11). We calculated  
100 phylogenetic signals in each of the measured characters using Blomberg's K (11) (SM10). To  
101 reconstruct the ancestral character states of nematocyst types and other categorical traits,  
102 we use stochastic character mapping (SIMMAP) using the package *phytools* (12).

103 In order to examine the phenotypic integration in the tentillum, we explored the correla-

104 tional structure among continuous characters and among their evolutionary histories using  
105 principal component analysis (PCA) and phylogenetic PCA (12). Since the character dataset  
106 contains many gaps due to missing characters and inapplicable states, we carried out these  
107 analyses on a subset of species and characters that allowed for the most complete dataset.  
108 This was done by removing the terminal filament characters (which are only shared by a small  
109 subset of species), and then removing species which had inapplicable states for the remaining  
110 characters (apolemiids and cystonects). In addition, we obtained the correlations between  
111 the phylogenetic independent contrasts (13) using the package *rphylip* (14). We identified  
112 four hypothetical modules among the tentillum characters: (1) The tentillum scaffold module  
113 – cnidoband length & width, nematocyst row number, pedicle & elastic strand width, tentacle  
114 width; (2) the heteroneme module – heteroneme length & width, shafts length & width; (3)  
115 the haploneme module – length and width; and (4) the terminal filament module – desmoneme  
116 & rhopaloneme length & width. To test and quantify phenotypic integration between these  
117 multivariate modules, we used the phylogenetic phenotypic integration test in the package  
118 *geomorph* (15).

119 When looking at the morphospace of species in different feeding guilds, we also used  
120 PCA on the complete tentacular character dataset transforming inapplicable states of absent  
121 characters to zeros to account for similarity based on character presence/absence. Using  
122 these principal components, we examined the occupation of the morphospace across species  
123 in different feeding guilds using a phylogenetic MANOVA with the package *geiger* (8) to  
124 assess the variation explained, and a morphological disparity test with the package *geomorph*  
125 (15) to assess differences in the extent occupied by each guild.

126 In order to detect and evaluate instances of convergent evolution, we used the package  
127 SURFACE (16). This tool identifies OU regimes and their optima given a tree and character  
128 data, and then evaluates where the same regime has appeared independently in different  
129 lineages. We applied these analyses to the haploneme nematocyst length and width characters  
130 as well as to the most complete dataset without inapplicable character states.

<sup>131</sup> In order to generate hypotheses on the diets of siphonophores using tentilla morphology,  
<sup>132</sup> we used the discriminant analyses of principal components (DAPC) trained in (4) using the  
<sup>133</sup> package *adegenet* (???) to predict the feeding guilds of species in the dataset for which there  
<sup>134</sup> are no published feeding observations.

<sup>135</sup> In order to observe the discharge behavior of different tentilla, we recorded high speed  
<sup>136</sup> footage (1000-3000 fps) of tentillum and nematocyst discharge by live siphonophore specimens  
<sup>137</sup> (26 species) using a Phantom Miro 320S camera mounted on a stereoscopic microscope. We  
<sup>138</sup> mechanically elicited tentillum and nematocyst discharge using a fine metallic pin. We used  
<sup>139</sup> the Phantom PCC software to analyze the footage. For the 10 species recorded, we measured  
<sup>140</sup> total cnidoband discharge time (ms), heteroneme filament length ( $\mu\text{m}$ ), and discharge speeds  
<sup>141</sup> (mm/s) for cnidoband, heteronemes, haplonemes, and heteroneme shafts when possible (data  
<sup>142</sup> available in the Dryad repository).

## <sup>143</sup> Results

<sup>144</sup> *Evolutionary history of tentillum morphology* – In (4), we produced the most speciose  
<sup>145</sup> siphonophore molecular phylogeny to date, while incorporating the most recent findings  
<sup>146</sup> in siphonophore deep node relationships. This phylogeny revealed for the first time that  
<sup>147</sup> the genus *Erenna* is the sister to *Stephanomia amphytridis*. *Erenna* and *Stephanomia* bear  
<sup>148</sup> the largest tentilla among all siphonophores, thus their monophyly indicates that there was  
<sup>149</sup> a single evolutionary transition to giant tentilla. Siphonophore tentilla range in size from  
<sup>150</sup> ~30  $\mu\text{m}$  in some *Cordagalma* specimens to 2-4 cm in *Erenna* species, and up to 8 cm in  
<sup>151</sup> *Stephanomia amphytridis* (17). Most siphonophore tentilla measure between 175 and 1007  
<sup>152</sup>  $\mu\text{m}$  (1st and 3rd quartiles), with a median of 373  $\mu\text{m}$ . The extreme gain of tentillum size in  
<sup>153</sup> this newly found clade may have important implications for access to large prey size classes  
<sup>154</sup> such as adult deep-sea fishes.

<sup>155</sup> Siphonophore tentilla are defined as lateral, monostichous evaginations of the tentacle  
<sup>156</sup> gastrovascular lumen with epidermal nematocysts (1). The buttons on *Physalia* tentacles

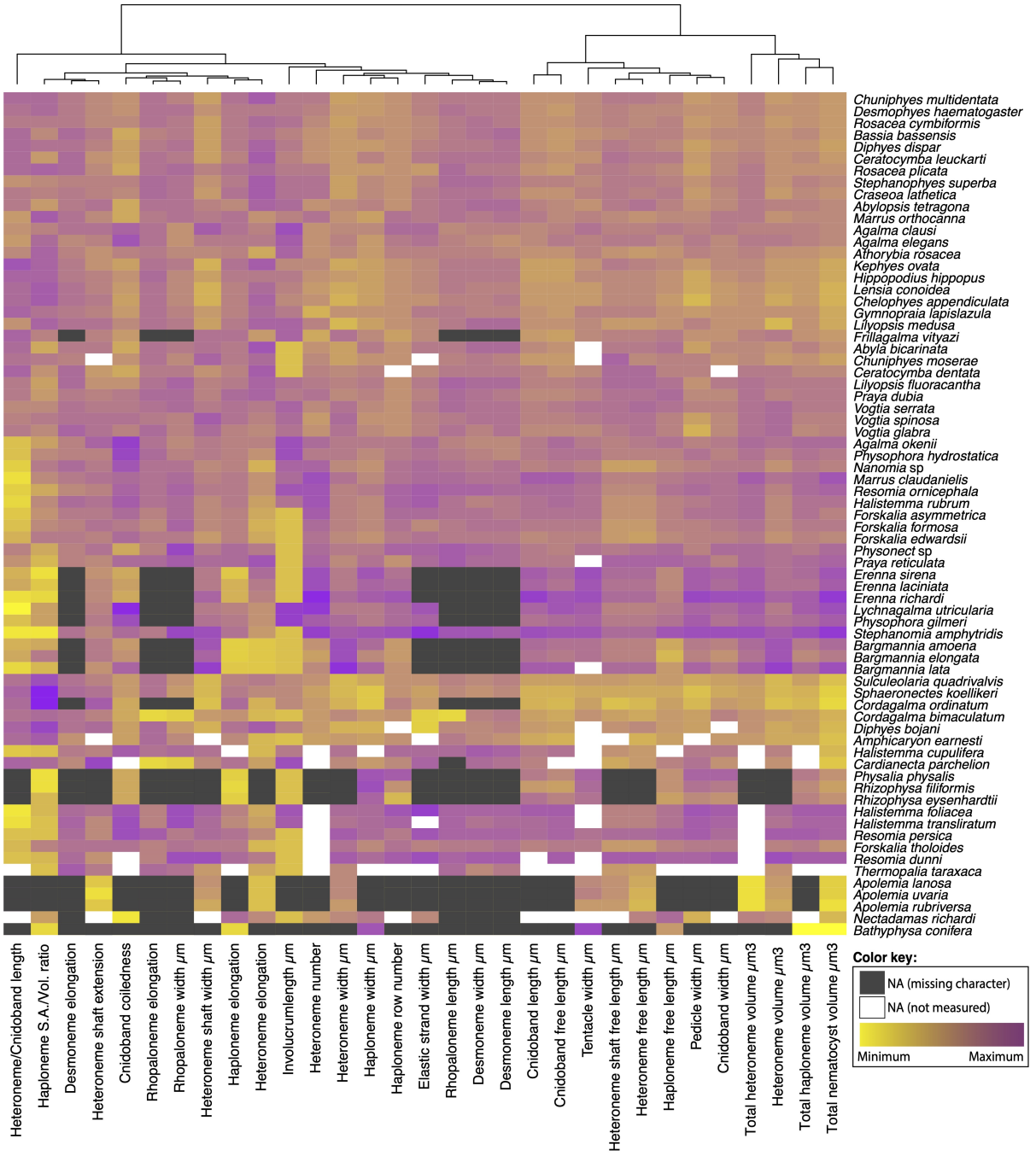


Figure 2: Heatmap summarizing the morphological diversity measured in Damian-Serrano *et al.* 2020 for 96 species of siphonophores clustered by similarity (raw data published in Damian-Serrano 2020). Missing values from absent characters presented as dark grey cells, missing values produced from technical difficulties presented as white cells. Values scaled by character.

157 were not traditionally regarded as tentilla, but (18) and our observations (3), confirm that the  
158 buttons contain evaginations of the gastrovascular lumen, thus satisfying all the criteria for  
159 the definition. In this light, and given that most Cystonectae bear conspicuous tentilla, we  
160 conclude (in agreement with (3) and (4)) that tentilla are likely ancestral to all siphonophores,  
161 and secondarily lost twice, once in *Apolemia* and again in *Bathyphysa conifera*.

162 In order to gain a broad perspective on the evolutionary history of tentilla, we reconstructed  
163 the phylogenetic positions of the main categorical character shifts using stochastic character  
164 mapping (SM1-9) and summarized in (Fig. 3). Some of these characters include the gain  
165 and loss of nematocyst types. Based on external information, we assume that haploneme  
166 nematocysts are ancestrally present in siphonophore tentacles since they are present in the  
167 tentacles of many other hydrozoans (5). Haplonemes first diverged into spherical isorhizas  
168 of 2 size classes in Cystonectae, and elongated anisorhizas of one size class in Codonophora.  
169 Haplonemes were likely lost in the tentacles of *Apolemia* but retained as spherical isorhizas in  
170 other *Apolemia* tissues (19). Similarly, while heteronemes exist in other tissues of cystonects,  
171 they appear in the tentacles of codonophorans exclusively, as birhopaloids in *Apolemia*,  
172 stenoteles in eucladophoran physonects, and microbasic mastigophores in calycophorans.

173 The clades defined in (4) are characterized by unique evolutionary innovations in their  
174 tentilla. The clade Eucladophora (containing Pyrostephidae, Euphysonectae, and Caly-  
175 cophorae) encompasses all of the extant Siphonophore species (178 of 186) except Cystonects  
176 and *Apolemia*. Innovations that arose along the stem of this group include spatially seg-  
177 regated heteroneme and haploneme nematocysts, terminal filaments, and elastic strands  
178 (Fig. 3). Pyrostephids evolved a unique bifurcation of the axial gastrovascular canal of  
179 the tentillum known as the “saccus” (1). The stem to the clade Tendiculophora (clade  
180 containing Euphysonectae and Calycophorae) subsequently acquired further novelties such  
181 as the desmoneme and rhopaloneme (acrophore subtype ancestral) nematocysts on the  
182 terminal filament (Fig. 3), which bears no other nematocyst type. These are arranged  
183 in sets of 2 parallel rhopalonemes for each single desmoneme (20, 21). The involucrum is

<sup>184</sup> an expansion of the epidermal layer that can cover part or all of the cnidoband (Fig. 1).  
<sup>185</sup> This structure, together with differentiated larval tentilla, appeared in the stem branch to  
<sup>186</sup> Clade A physonects. Calycophorans evolved novelties such as larger desmonemes at the  
<sup>187</sup> distal end of the cnidoband, pleated pedicles with a “hood” (here considered homologous  
<sup>188</sup> to the involucrum) at the proximal end of the tentillum, anacrophore rhopalonemes, and  
<sup>189</sup> microbasic mastigophore-type heteronemes. While calycophorans have diversified into most  
<sup>190</sup> of the extant described siphonophore species (108 of 186), their tentilla have not undergone  
<sup>191</sup> any major categorical gains or losses since their most recent common ancestor. Nonetheless,  
<sup>192</sup> they have evolved a wide variation in nematocyst and cnidoband sizes. Ancestrally (and  
<sup>193</sup> retained in most prayomorphs and hippopodids), the calycophoran tentillum is recurved  
<sup>194</sup> where the proximal and distal ends of the cnidoband are close together. Diphyomorph tentilla  
<sup>195</sup> are slightly different in shape, with straighter cnidobands.

<sup>196</sup> *Evolution of tentillum and nematocyst characters* – One-third of the characters measured  
<sup>197</sup> in (4) support a non-phylogenetic generative model, indicating they are not phylogenetically  
<sup>198</sup> conserved (SM10). Most (74%) characters present a significant phylogenetic signal, yet only  
<sup>199</sup> total nematocyst volume, haploneme length, and heteroneme-to-cnidoband length ratio had  
<sup>200</sup> a phylogenetic signal with K larger than 1. Total nematocyst volume and cnidoband-to-  
<sup>201</sup> heteroneme length ratio showed strongly conserved phylogenetic signals. The majority (67%)  
<sup>202</sup> of characters support BM models, indicating a history of neutral constant divergence. We did  
<sup>203</sup> not find any relationship between phylogenetic signal and BM model support. Haploneme  
<sup>204</sup> nematocyst length was the only character with support for an EB model of decreasing rate  
<sup>205</sup> of evolution with time. No character had support for a single-optimum OU model (when  
<sup>206</sup> not informed by feeding guild regime priors).

<sup>207</sup> *Evolution of nematocyst shape* – The greatest evolutionary change in haploneme nemato-  
<sup>208</sup> cyst shape occurred in a single shift towards elongation in the stem of Tendiculophora, which  
<sup>209</sup> contains the majority of described siphonophore species other than Cystonects, *Apolemia*,  
<sup>210</sup> and Pyrostephidae. There is one secondary return to more oval, less elongated haplonemes in

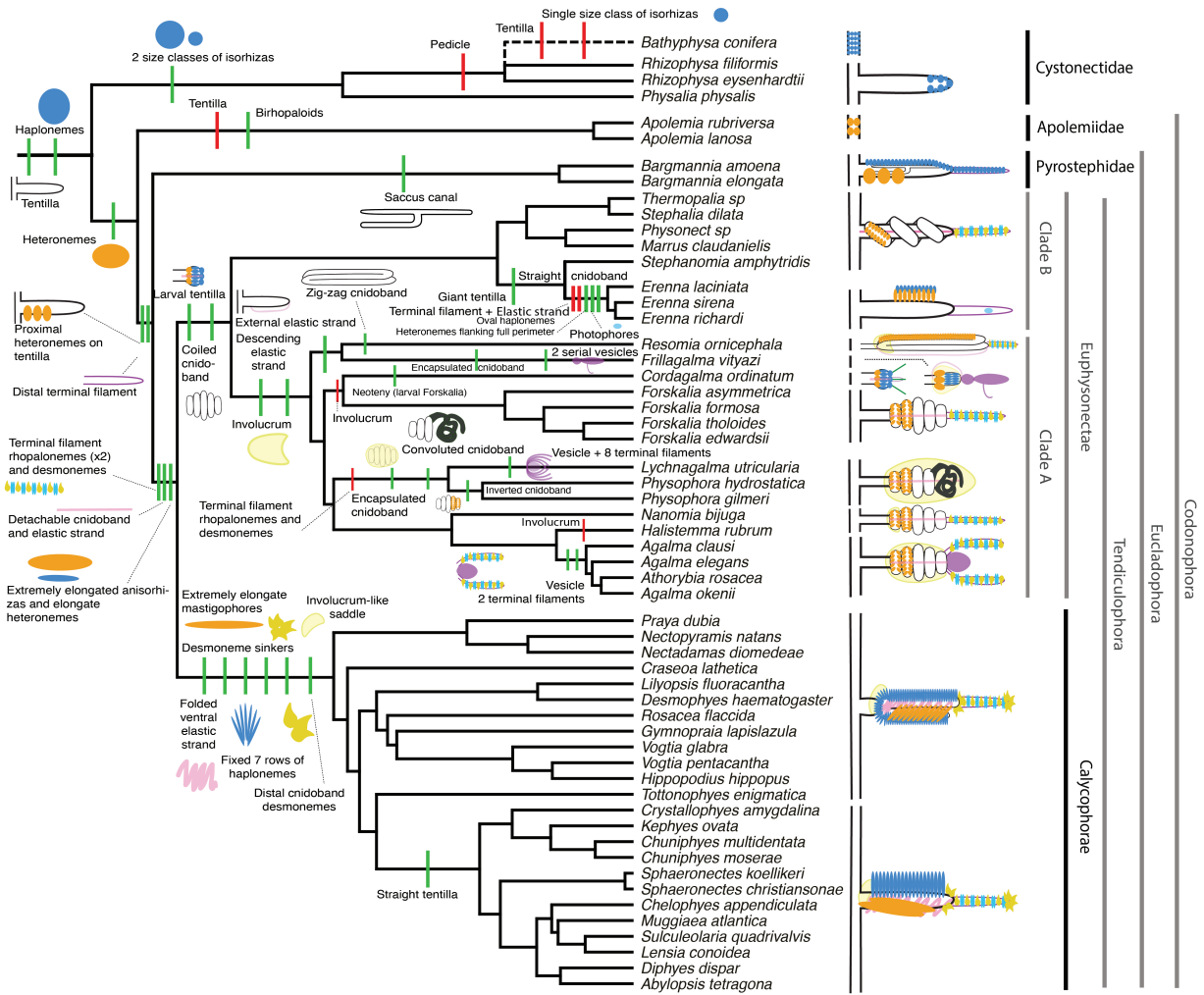


Figure 3: Siphonophore cladogram with the main categorical character gains (green) and losses (red) mapped. Some branch lengths were modified from the Bayesian chronogram to improve readability. The main visually distinguishable tentillum types are sketched next to the species that bear them, showing the location and arrangement of the main characters. In large, complex-shaped euphysonect tentilla, haplonemes were omitted for simplification. The hypothesized phylogenetic placement of the rhizophysid *Bathyphysa conifera* branch was appended manually as a polytomy (dashed line).

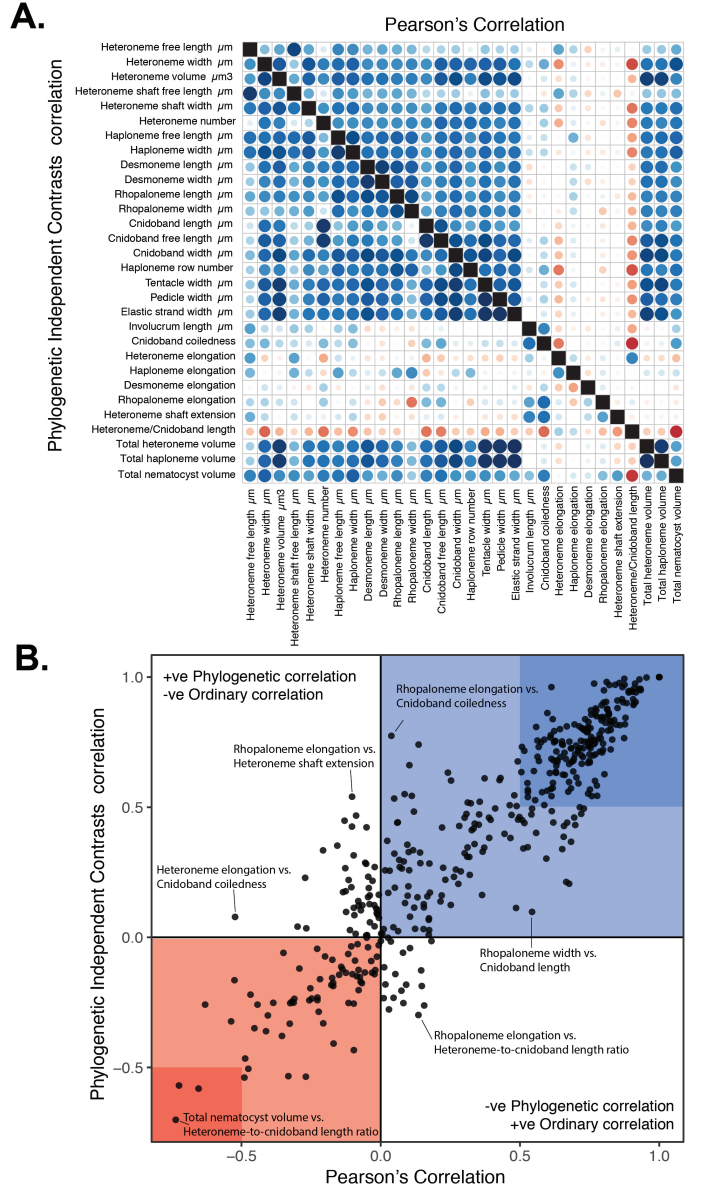


Figure 4: A. Correlogram showing strength of ordinary (upper triangle) and phylogenetic (lower triangle) correlations between characters. Both size and color of the circles indicate the strength of the correlation ( $R^2$ ). B. Scatterplot of phylogenetic correlation against ordinary correlation showing a strong linear relationship ( $R^2 = 0.92$ , 95% confidence between 0.90 and 0.93). Light red and blue boxes indicate congruent negative and positive correlations respectively. Darker red and blue boxes indicate strong ( $<-0.5$  or  $>0.5$ ) negative and positive correlation coefficients respectively.

*Erenna*, but it does not reach the sphericity present in Cystonectae or Pyrostephidae (Fig. 5). Heteroneme evolution presents a less discrete evolutionary history, where Tendiculophora evolved more elongate heteronemes, but the difference between theirs and other siphonophores is much smaller than the variation in shape within Tendiculophora, bearing no phylogenetic signal. In this clade, the evolution of heteroneme shape has diverged in both directions, and there is no correlation with haploneme shape (Fig. 5), which has remained fairly constant (elongation between 1.5 and 2.5). Haploneme and heteroneme shape share 21% of their variance across extant values, and 53% of the variance in their shifts along the branches of the phylogeny. However, much of this correlation is due to the sharp contrast between Pyrostephidae and their sister group Tendiculophora. We searched for regime shifts in the evolution of haploneme nematocyst shape characters using a SURFACE (16). SURFACE identified seven distinct OU regimes in the evolutionary history of haploneme length and width (Fig. 8A). The different regimes are located (1) in cystonects, (2) in pyrostephids, (7) in apolemiids, (9) in *Erenna*, (6) in *Stephanomia*, (3) in most of Tendiculophora, (5) in *Cordagalma ordinatum*, (4) in most diphyomorphs, and (8) in *Abylopsis tetragona* and *Diphyes dispar*.

*Phenotypic integration of the tentillum* – Phenotypically integrated structures maintain evolutionary correlations between its constituent characters. Of the phylogenetic correlations (Fig. 4a, lower triangle), 81.3% were positive and 18.7% were negative, while of the ordinary correlations (Fig. 4a, upper triangle) 74.6% were positive and 25.4% were negative. Half (49.9%) of phylogenetic correlations were  $>0.5$ , while only 3.6% are  $< -0.5$ . Similarly, among the correlations across extant species, 49.1% were  $>0.5$  and only 1.5% were  $< -0.5$ . In addition, we found that 13.9% of character pairs had opposing phylogenetic and ordinary correlation coefficients. Just 4% have negative phylogenetic and positive ordinary correlations (such as rhopaloneme elongation  $\sim$  heteroneme-to-cnidoband length ratio and haploneme elongation, or haploneme elongation  $\sim$  heteroneme number), and only 9.9% of character pairs had positive phylogenetic correlation yet negative ordinary correlation (such as heteroneme

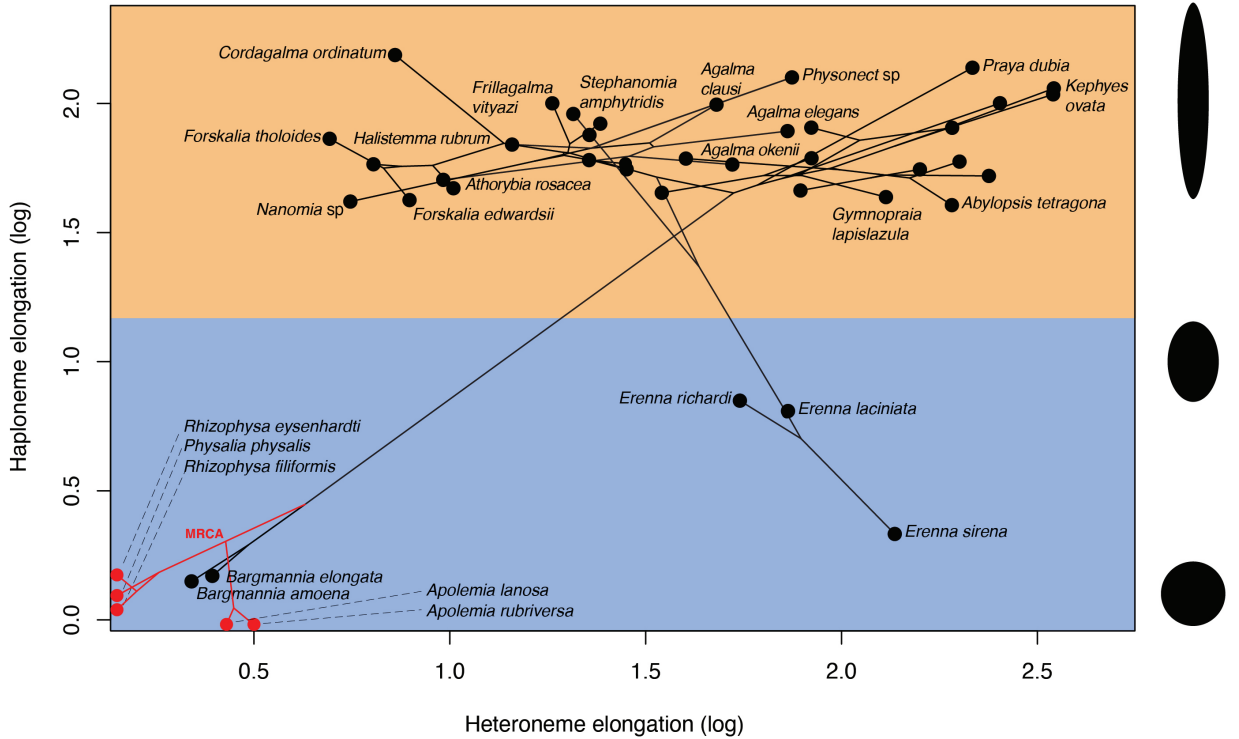


Figure 5: Phylomorphospace showing haploneme and heteroneme elongation (log scaled). Orange area delimits rod-shaped haplonemes, the blue area covers oval and round-shaped haplonemes. Smaller dots and lines represent phylogenetic relationships and ancestral states of internal nodes under BM. Species nodes in red lack either haplonemes or heteronemes, and their values are projected onto the axis of the nematocyst type they bear. Cystonects have no tentacle heteronemes and are projected onto the haploneme axis. Apolemiids have no tentacle haplonemes and are projected onto the heteroneme axis.

238 elongation ~ cnidoband convolution and involucrum length, or rhopaloneme elongation with  
239 cnidoband length). These disparities could be explained by Simpson's paradox (22): the  
240 reversal of the sign of a relationship when a third variable (or a phylogenetic topology  
241 (23)) is considered. However, no character pair had correlation coefficient differences larger  
242 than 0.64 between ordinary and phylogenetic correlations (heteroneme shaft extension ~  
243 rhopaloneme elongation has a Pearson's correlation of 0.10 and a phylogenetic correlation  
244 of -0.54). Rhopaloneme elongation shows the most incongruencies between phylogenetic  
245 and ordinary correlations with other characters. The phenotypic integration test showed  
246 significant integration signal between all modules, tentillum and haploneme modules sharing  
247 the greatest regression coefficient (SM12).

248 In the non-phylogenetic PCA morphospace using only simple characters (Fig. 6), PC1  
249 (aligned with tentillum and tentacle size) explained 69.3% of the variation in the tentillum  
250 morphospace, whereas PC2 (aligned with heteroneme length, heteroneme number, and  
251 haploneme arrangement) explained 13.5%. In a phylogenetic PCA, 63% of the evolutionary  
252 variation in the morphospace is explained by PC1 (aligned with shifts in tentillum size), while  
253 18% is explained by PC2 (aligned with shifts in heteroneme number and involucrum length).

254 *Morphospace occupation* – In order to examine the occupation structure of the morphospace  
255 across all siphonophore species in the dataset, we cast a PCA on the data after transforming  
256 inapplicable states (due to absence of character) to zeroes. This allows us to accommodate  
257 species with many missing characters (such as cystonects or apolemiids), and to account for  
258 common absences as morphological similarities. In this ordination, PC1 explains 47.45%  
259 of variation (aligned with cnidoband size) and PC2 explains 16.73% of variation (aligned  
260 with heteroneme volume and involucrum). When superimposing feeding guilds onto the  
261 morphospace (Fig. 7), we find that the morphospaces of each feeding guild are only slightly  
262 overlapping in PC1 and PC2. A phylogenetic MANOVA showed that feeding guilds explain  
263 27.63% of variance across extant species ( $p$  value < 0.000001), and 20.97% of the variance  
264 in the tree species accounting for phylogeny, an outcome significantly distinct from the

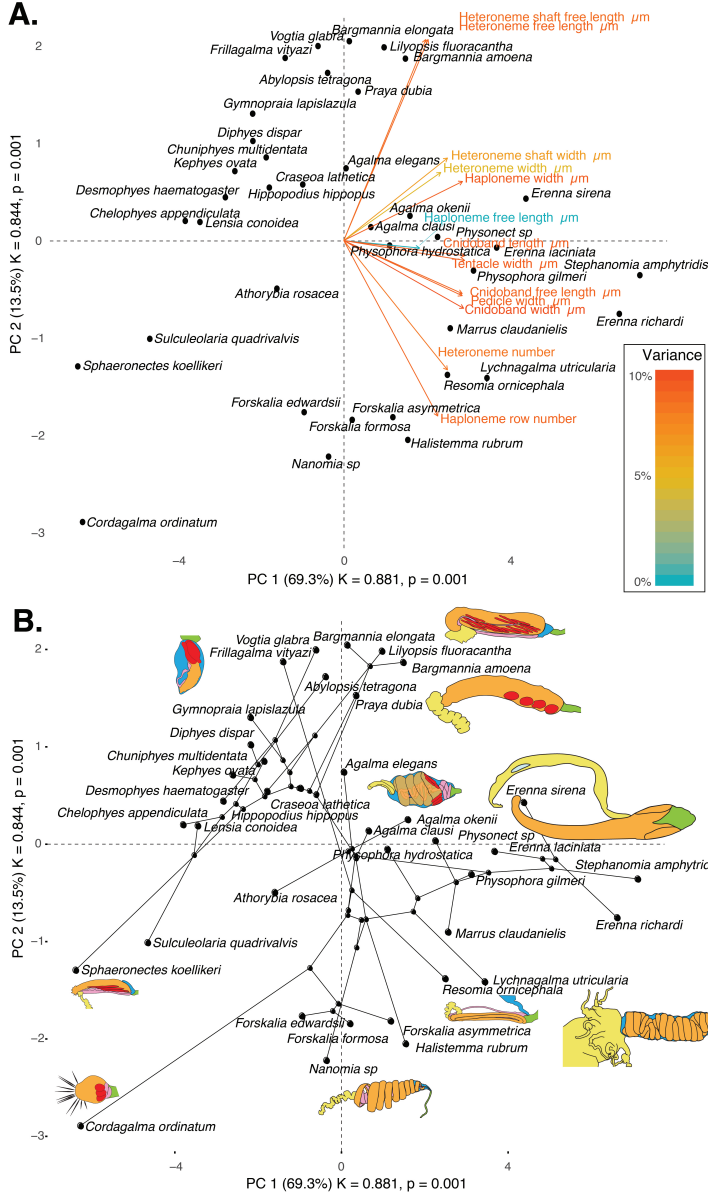


Figure 6: Phylomorphospace of the simple continuous characters principal components, excluding ratios and composite characters. A. Variance explained by each variable in the PC1-PC2 plane. Axis labels include the phylogenetic signal (K) for each component and p-value. B. Phylogenetic relationships between the species points distributed in that same space.

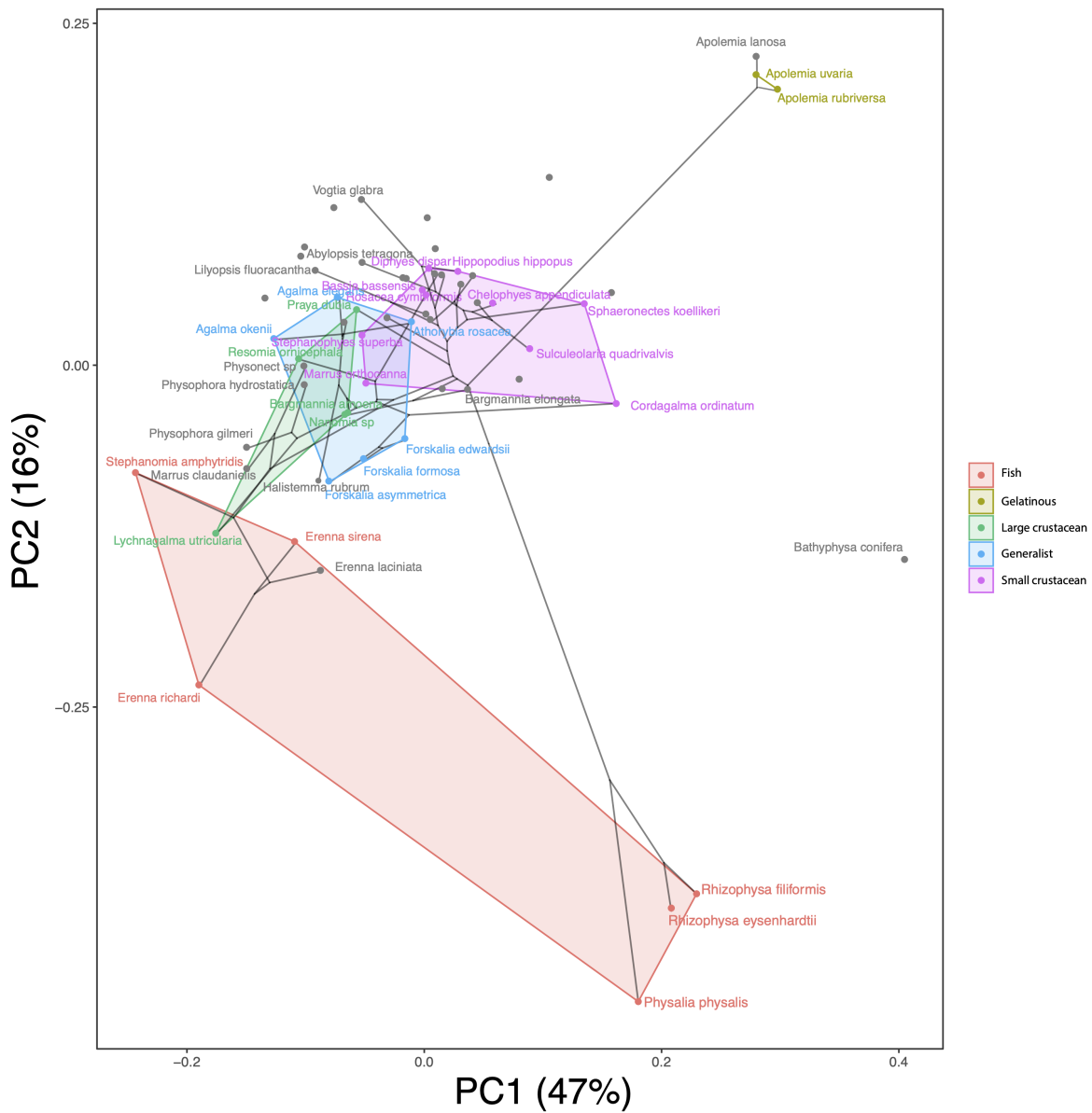


Figure 7: Phylomorphospace showing PC1 and PC2 from a PCA of continuous morphological characters with inapplicable states transformed to zeroes, overlapped with polygons conservatively defining the space occupied by each feeding guild. Lines between species coordinates show the phylogenetic relationships between them.

expectation under neutral evolution ( $p$ -value = 0.0196). In addition, a morphological disparity analysis accounting for phylogenetic structure shows that the morphospace of fish specialists is significantly broader than that of generalists and other specialists. This is due to the large morphological disparities between cystonects and piscivorous euphysonects. There are no significant differences among the morphospace disparities of the other feeding guilds.

*Convergent evolution* – Convergence is a widespread evolutionary phenomenon where distantly related clades independently evolve similar phenotypes. Using the package SURFACE (16), we identified convergence in haploneme nematocyst shape and in morphospace position. In (4), we identified haploneme nematocyst shape as one of the traits associated with the convergent evolution of piscivory. Here we find that indeed wider haploneme nematocysts have convergently evolved in the piscivore cytonects and *Erenna* spp. (Fig. 8A). Extremely narrow haplonemes have also evolved convergently in *Cordagalma ordinatum* and copepod specialist calycophorans such as *Sphaeronectes koellikeri*. When integrating many traits into a couple principal components, we find two distinct convergences between euphysonects and calycophorans with a reduced prey capture apparatus. Those convergences are between *Frillagalma vityazi* and calycophorans, and once again between *Cordagalma ordinatum* and *Sphaeronectes koellikeri* (Fig. 8B).

*Functional morphology of tentillum and nematocyst discharge* – Tentillum and nematocyst discharge high speed measurements are available in the Dryad repository. While the sample sizes of these measurements were insufficient to draw reliable statistical results at a phylogenetic level, we did observe patterns that may be relevant to their functional morphology. For example, cnidoband length is strongly correlated with discharge speed ( $p$  value = 0.0002). This is probably the sole driver of the considerable difference between euphysonect and calycophoran tentilla discharge speeds (average discharge speeds: 225.0mm/s and 41.8mm/s respectively; t-test  $p$  value = 0.011), since the euphysonects have larger tentilla than the calycophorans among the species recorded. In addition, we observed that calycophoran haploneme tubules fire faster than those of euphysonects (T-test  $p$  value = 0.001). Haploneme

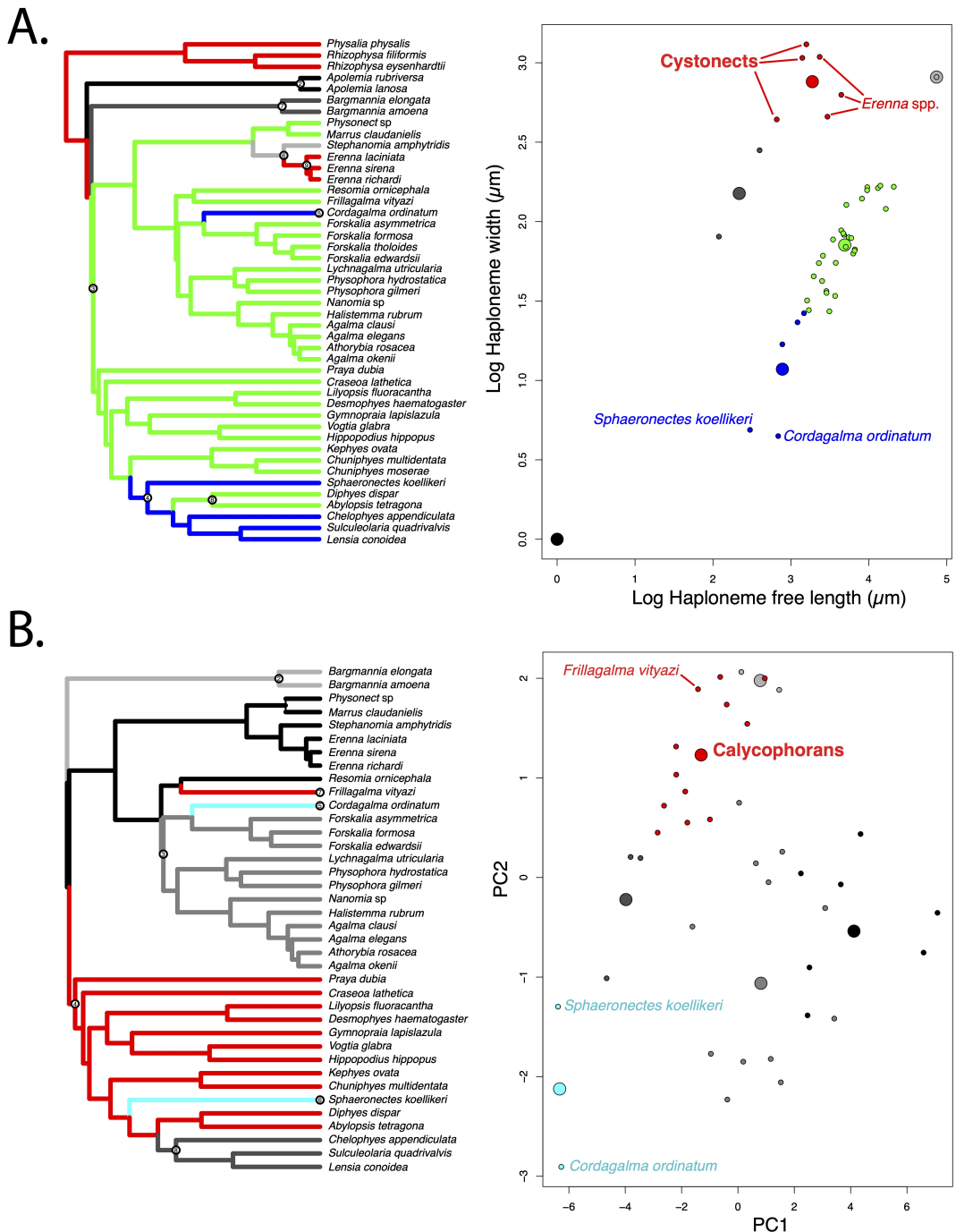


Figure 8: SURFACE plots showing convergent evolutionary regimes modelled under OU for (A) haploneme nematocyst length & width, and (B) for PC1 & 2 of all continuous characters with the exception of terminal filament nematocysts, and removing taxa with inapplicable character states. Node numbers on the tree label different regimes, regimes of the same color are identified as convergent. Small circles on the scatterplots indicate species values, large circles indicate the average position of the OU optima ( $\theta$ ) for a given combination of convergent regimes.

292 nematocysts discharge 2.8x faster than heteroneme nematocysts (T-test p value = 0.0012).  
293 Finally, we observed that the stenoteles of the Euphysonectae discharge a helical filament  
294 that “drills” itself through the medium it penetrates as it everts.

295 *Generating dietary hypotheses using tentillum morphology* – For many siphonophore species,  
296 no feeding observations have yet been published. To help bridge this gap of knowledge,  
297 we generated hypotheses about the diets of these understudied siphonophores based on  
298 their known tentacle morphology using one the linear discriminant analyses of principal  
299 components (DAPC) fitted in (4). This provides concrete predictions to be tested in  
300 future work and helps extrapolate our findings to many poorly known species that are  
301 extremely difficult to collect and observe. The discriminant analysis for feeding guild (7  
302 principal components, 4 discriminants) produced 100% discrimination, and the highest loading  
303 contributions were found for the characters (ordered from highest to lowest): Involutrum  
304 length, heteroneme volume, heteroneme number, total heteroneme volume, tentacle width,  
305 heteroneme length, total nematocyst volume, and heteroneme width. We used the predictions  
306 from this discriminant function to generate hypotheses about the feeding guild of 45 species  
307 in the morphological dataset. This extrapolation predicts that two other *Apolemia* species are  
308 gelatinous prey specialists like *Apolemia rubriversa*, and predicts that *Erenna laciniata* is a  
309 fish specialist like *Erenna richardi*. When predicting soft- and hard-bodied prey specialization,  
310 the DAPC achieved 90.9% discrimination success, only marginally confounding hard-bodied  
311 specialists with generalists (SM13). The main characters driving this discrimination are  
312 involutrum length, heteroneme number, heteroneme volume, tentacle width, total nematocyst  
313 volume, total haploneme volume, elastic strand width, and heteroneme length.

## 314 Discussion

315 *On the evolution of tentilla morphology* – *On the evolution of tentilla morphology* – The  
316 evolutionary rate covariance results in (4) indicate that tentilla are not only phenotypically  
317 integrated but also show patterns of evolutionary modularity, where different sets of characters

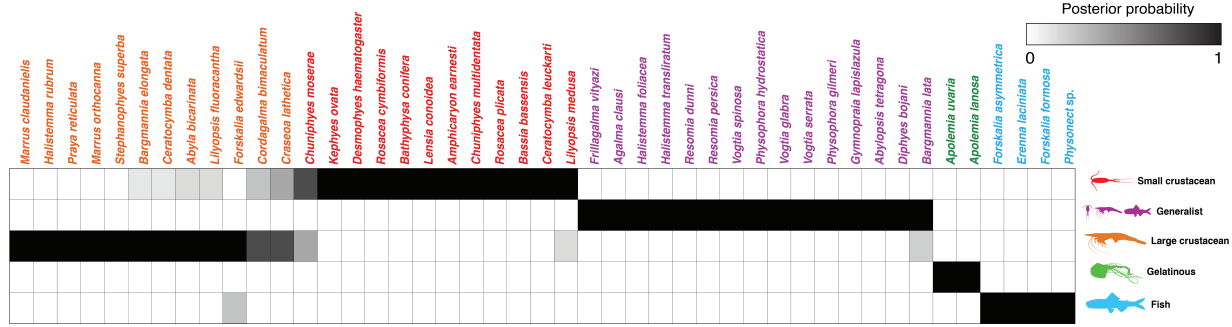


Figure 9: Hypothetical feeding guilds for siphonophore species predicted by a 6 PCA DAPC. Cell darkness indicates the posterior probability of belonging to each guild. Training data set transformed so inapplicable states are computed as zeroes. Species ordered and colored according to their predicted feeding guild.

318 appear to evolve in stronger correlations among each other than with other characters  
 319 (24). This may be indicative of the underlying genetic and developmental dependencies  
 320 among closely homologous nematocyst types (such as desmonemes and rhopalonemes) and  
 321 structures. The rate covariance results are congruent with the evolutionary correlations we  
 322 found (Fig. /ref(figure8)). In addition, these evolutionary modules point to hypothetical  
 323 functional modules. For example, the coiling degree of the cnidoband and the extent of the  
 324 involucrum have correlated rates of evolution, while high-speed videos (pers. obs.) show that  
 325 the involucrum helps direct the whiplash of the uncoiling cnidoband distally (towards the  
 326 prey). The clade Tendiculophora contains far more species than its relatives Cystonectae,  
 327 Apolemiidae, and Pyrostephidae. An increase in clade richness and ecological diversification  
 328 can be triggered by a ‘key innovation’ (25). The evolutionary innovation of the Tendiculophora  
 329 tentilla with shooting cnidobands and modular regions may have facilitated further dietary  
 330 diversification. A specific instance of this may have been the access to the abundant small  
 331 crustacean prey such as copepods. The rapid darting escape response of copepods may  
 332 preclude their capture in siphonophores without shooting cnidobands.

333 The siphonophore tentillum morphospace has a fairly low extant dimensionality due  
 334 to having an evolutionary history with many synchronous, correlated changes. This is  
 335 consistent with strong phenotypic integration where genetic and developmental correlations

336 are maintained by natural selection to preserve a complex function across the wide variety  
337 of morphologies present. Since most tentillum characters develop from a common bud  
338 (budding tentilla near the base of the tentacle), structural correlations are expected. Similarly,  
339 correlations between the features of different nematocyst subtypes within a species are also  
340 expected given their common evolutionary and developmental origin (26, 27). However, we  
341 also found correlations between nematocyst and tentillum characters. Siphonophore tentacle  
342 nematocysts (in their cnidocytes) are not produced nor matured in the developing tentillum.  
343 These cnidocytes are produced by dividing cnidoblasts in the basigaster (basal swelling of  
344 the gastrozooid). Once the cnidocytes have assembled the nematocyst, they migrate outward  
345 along the tentacle (28) and position themselves in the tentillum according to their type and size  
346 (20). Thus, the developmental programs that produce the observed nematocyst morphologies  
347 are spatially separated from those producing the tentillum morphologies. Therefore, we  
348 hypothesize the genetic correlations and phenotypic integration between tentillum and  
349 nematocyst characters are maintained through natural selection on separate regulatory  
350 networks, out of the necessity to work together and meet the spatial, mechanical, and  
351 functional constraints of their prey capture behavior.

352 *Heterochrony and convergence in the evolution of tentilla with diet* - In addition to  
353 identifying shifts in prey type, (4)revealed the specific morphological changes in the prey  
354 capture apparatus associated with these changes. Copepod-specialized diets have evolved  
355 independently in *Cordagalma* and some calycophorans. These evolutionary transitions  
356 happened together with transitions to smaller tentilla with fewer and smaller cnidoband  
357 nematocysts. We found that these morphological transitions evolved convergently in these taxa.  
358 Tentilla are expensive single-use structures (6), therefore we would expect that specialization  
359 in small prey would beget reductions in the size of the prey capture apparatus to the minimum  
360 required for the ecological performance. Such a reduction in size would require extremely  
361 fast rates of trait evolution in an ordinary scenario. However, *Cordagalma*'s tentilla strongly  
362 resemble the larval tentilla (only found in the first-budded feeding body of the colony) of

their sister genus *Forskalia*. This indicates that the evolution of *Cordagalma* tentilla could be a case of paedomorphic heterochrony associated with predatory specialization on smaller prey. This developmental shift may have provided a shortcut for the evolution of a smaller prey capture apparatus.

Our work identifies yet another novel example of convergent evolution. The region of the tentillum morphospace (Fig. /???(figure9) & Fig. /ref(surface)B) occupied by calycophorans was independently (and more recently) occupied by the physonect *Frillagalma vityazi*. Like calycophorans, *Frillagalma* tentilla have small C-shaped cnidobands with a few rows of anisorhizas. Unlike calycophorans, they lack paired elongate microbasic mastigophores. Instead, they bear exactly three oval stenoteles, and their cnidobands are followed by a branched vesicle, unique to this genus. Their tentillum morphology is very different from that of other related physonects, which tend to have long, coiled, cnidobands with many paired oval stenoteles. Our SURFACE analysis clearly indicates a regime convergence in the cnidoband morphospace between *Frillagalma* and calycophorans (Fig. /???(surface)B). Most studies on calycophoran diets have reported their prey to be primarily composed of small crustaceans, such as copepods or ostracods (7, 29). The diet of *Frillagalma vityazi* is unknown, but this morphological convergence suggests that they evolved to capture similar kinds of prey. The DAPCs in (4) predict that *Frillagalma* has a generalist niche with both soft and hard-bodied prey, including copepods.

*Evolution of nematocyst shape* – A remarkable feature of siphonophore haplonemes is that they are outliers to all other Medusozoa in their surface area to volume relationships, deviating significantly from sphericity (30). This suggests a different mechanism for their discharge that could be more reliant on capsule tension than on osmotic potentials (31), and strong selection for efficient nematocyst packing in the cnidoband (20, 30). Our results show that Codonophora underwent a shift towards elongation and Cystonectae towards sphericity, assuming the common ancestor had an intermediate state. Since we know that the haplonemes of other hydrozoan outgroups are generally spheroid, it is more parsimonious

390 to assume that cystonects are simply retaining this ancestral state. Later, we observe a  
391 return to more rounded (ancestral) haplonemes in *Erenna*, concurrent with a secondary gain  
392 of a piscivorous trophic niche, like that exhibited by cystonects. Our SURFACE analysis  
393 shows that this transition to roundness is convergent with the regime occupied by cystonects  
394 (Fig. /????(surface)A). Purcell (29) showed that haplonemes have a penetrating function  
395 as isorhizas in cystonects and an adhesive function as anisorrhizas in Tendiculophora. It is  
396 no coincidence that the two clades that have converged to feed primarily on fish have also  
397 converged morphologically toward more compact haplonemes. Isorhizas in cystonects are  
398 known to penetrate the skin of fish during prey capture, and to deliver the toxins that aid in  
399 paralysis and digestion (32). *Erenna*'s anisorrhizas are also able to penetrate human skin and  
400 deliver a painful sting (33) (and pers. obs.), a common feature of piscivorous cnidarians like  
401 the Portuguese man-o-war or box jellies.

402 The implications of these results for the evolution of nematocyst function are that an  
403 innovation in the discharge mechanism of haplonemes may have occurred during the main shift  
404 to elongation. Elongate nematocysts can be tightly packed into cnidobands. We hypothesize  
405 this may be a Tendiculophora lineage-specific adaptation to packing more nematocysts into a  
406 limited tentillum space, as suggested by (20). Thomason (30) hypothesized that smaller, more  
407 spherical nematocysts, with a lower surface area to volume ratio, are more efficient in osmotic-  
408 driven discharge and thus have more power for skin penetration. The elongated haplonemes  
409 of crustacean-eating Tendiculophora have never been observed penetrating their crustacean  
410 prey (29), and are hypothesized to entangle the prey through adhesion of the abundant  
411 spines to the exoskeletal surfaces and appendages. Entangling requires less acceleration and  
412 power during discharge than penetration, as it does not rely on point pressure. In fish-eating  
413 cystonects and *Erenna* species, the haplonemes are much less elongated and very effective at  
414 penetration, in congruence with the osmotic discharge hypothesis. Tendiculophora, composed  
415 of the clades Euphysonectae and Calycophorae, includes the majority of siphonophore species.  
416 Within these clades are the most abundant siphonophore species, and a greater morphological

417 and ecological diversity is found. We hypothesize that this packing-efficient haploneme  
418 morphology may have also been a key innovation leading to the diversification of this clade.  
419 However, other characters that shifted concurrently in the stem of this clade could have been  
420 equally responsible for their extant diversity.

421 *Generating hypotheses on siphonophore feeding ecology* – One motivation for our research  
422 is to understand the links between predator capture tools and their diets so we can generate  
423 hypotheses about the diets of siphonophores based on morphological characteristics. Indeed,  
424 our discriminant analyses were able to distinguish between different siphonophore diets  
425 based on morphological characters alone. The models produced by these analyses generated  
426 testable predictions about the diets of many species for which we only have morphological  
427 data of their tentacles. While the limited dataset used here is informative for generating  
428 tentative hypotheses, the empirical dietary data are still scarce and insufficient to cast robust  
429 predictions. This reveals the need to extensively characterize siphonophore diets and feeding  
430 habits. In future work, we will test these ecological hypotheses and validate these models  
431 by directly characterizing the diets of some of those siphonophore species. Predicting diet  
432 using morphology is a powerful tool to reconstruct food web topologies from community  
433 composition alone. In many of the ecological models found in the literature, interactions  
434 among the oceanic zooplankton have been treated as a black box (34). The ability to predict  
435 such interactions, including those of siphonophores and their prey, will enhance the taxonomic  
436 resolution of nutrient-flow models constructed from plankton community composition data.

## 437 Acknowledgements

438 This work was supported by the Society of Systematic Biologists (Graduate Student Award  
439 to A.D.S.); the Yale Institute of Biospheric Studies (Doctoral Pilot Grant to A.D.S.); and  
440 the National Science Foundation (Waterman Award to C.W.D., and NSF-OCE 1829835 to  
441 C.W.D., S.H.D.H., and C. Anela Choy). A.D.S. was supported by a Fulbright Spain Graduate  
442 Studies Scholarship.

443 **References**

- 444 1. Totton AK, Bargmann HE (1965) *A synopsis of the siphonophora* (British Museum  
445 (Natural History)).
- 446 2. Mapstone GM (2014) Global diversity and review of siphonophorae (cnidaria: Hydro-  
447 zoa). *PLoS One* 9(2):e87737.
- 448 3. Munro C, et al. (2018) Improved phylogenetic resolution within siphonophora (cnidaria)  
449 with implications for trait evolution. *Molecular Phylogenetics and Evolution*.
- 450 4. Damian-Serrano A, Haddock SH, Dunn CW (2019) The evolution of siphonophore  
451 tentilla as specialized tools for prey capture. *bioRxiv*:653345.
- 452 5. Mariscal RN (1974) Nematocysts.
- 453 6. Mackie GO, Pugh PR, Purcell JE (1987) Siphonophore Biology. *Advances in Marine  
454 Biology* 24:97–262.
- 455 7. Purcell J (1981) Dietary composition and diel feeding patterns of epipelagic  
456 siphonophores. *Marine Biology* 65(1):83–90.
- 457 8. Harmon LJ, Weir JT, Brock CD, Glor RE, Challenger W (2007) GEIGER: Investigating  
458 evolutionary radiations. *Bioinformatics* 24(1):129–131.
- 459 9. Sugiura N (1978) Further analysts of the data by akaike's information criterion  
460 and the finite corrections: Further analysts of the data by akaike's. *Communications in  
461 Statistics- Theory and Methods* 7(1):13–26.
- 462 10. Pennell MW, FitzJohn RG, Cornwell WK, Harmon LJ (2015) Model adequacy and the  
463 macroevolution of angiosperm functional traits. *The American Naturalist* 186(2):E33–E50.
- 464 11. Blomberg SP, Garland T, Ives AR (2003) Testing for phylogenetic signal in comparative  
465 data: Behavioral traits are more labile. *Evolution* 57(4):717–745.
- 466 12. Revell LJ (2012) Phytools: An r package for phylogenetic comparative biology (and  
467 other things). *Methods in Ecology and Evolution* 3(2):217–223.
- 468 13. Felsenstein J (1985) Phylogenies and the comparative method. *The American  
469 Naturalist* 125(1):1–15.

- 470        14. Revell LJ, Chamberlain SA (2014) Rphylip: An r interface for phylip. *Methods in*  
471        *Ecology and Evolution* 5(9):976–981.
- 472        15. Adams DC, Collyer M, Kalliontzopoulou A, Sherratt E (2016) Geomorph: Software  
473        for geometric morphometric analyses.
- 474        16. Ingram T, Mahler DL (2013) SURFACE: Detecting convergent evolution from  
475        comparative data by fitting ornstein-uhlenbeck models with stepwise akaike information  
476        criterion. *Methods in ecology and evolution* 4(5):416–425.
- 477        17. Pugh P, Baxter E (2014) A review of the physonect siphonophore genera halistemma  
478        (family agalmatidae) and stephanomia (family stephanomiidae). *Zootaxa* 3897(1):1–111.
- 479        18. Bardi J, Marques AC (2007) Taxonomic redescription of the portuguese man-of-war,  
480        physalia physalis (cnidaria, hydrozoa, siphonophorae, cystonectae) from brazil. *Iheringia*  
481        *Série Zoologia* 97(4):425–433.
- 482        19. Siebert S, Pugh PR, Haddock SH, Dunn CW (2013) Re-evaluation of characters in  
483        apolemiidae (siphonophora), with description of two new species from monterey bay, california.  
484        *Zootaxa* 3702(3):201–232.
- 485        20. Skaer R (1988) *The formation of cnidocyte patterns in siphonophores* (Academic  
486        Press New York).
- 487        21. Skaer R (1991) Remodelling during the development of nematocysts in a siphonophore.  
488        *Hydrobiologia* (Springer), pp 685–689.
- 489        22. Blyth CR (1972) On simpson’s paradox and the sure-thing principle. *Journal of the*  
490        *American Statistical Association* 67(338):364–366.
- 491        23. Uyeda JC, Zenil-Ferguson R, Pennell MW (2018) Rethinking phylogenetic comparative  
492        methods. *Systematic Biology* 67(6):1091–1109.
- 493        24. Wagner GP (1996) Homologues, natural kinds and the evolution of modularity.  
494        *American Zoologist* 36(1):36–43.
- 495        25. Simpson GG (1955) *Major features of evolution* (Columbia University Press: New  
496        York).

- 497        26. Bode H (1988) Control of nematocyte differentiation in hydra. *The Biology of*  
498 *Nematocysts* (Elsevier), pp 209–232.
- 499        27. David CN, et al. (2008) Evolution of complex structures: Minicollagens shape the  
500 cnidarian nematocyst. *Trends in genetics* 24(9):431–438.
- 501        28. Carré D (1972) Study on development of cnidocysts in gastrozooids of muggiaeae kochi  
502 (will, 1844) (siphonophora, calycophora). *Comptes Rendus Hebdomadaires des Seances de*  
503 *l'Academie des Sciences Serie D* 275(12):1263.
- 504        29. Purcell JE (1984) The functions of nematocysts in prey capture by epipelagic  
505 siphonophores (coelenterata, hydrozoa). *The Biological Bulletin* 166(2):310–327.
- 506        30. Thomason J (1988) The allometry of nematocysts. *The Biology of Nematocysts*  
507 (Elsevier), pp 575–588.
- 508        31. Carré D, Carré C (1980) On triggering and control of cnidocyst discharge. *Marine &*  
509 *Freshwater Behaviour & Phy* 7(1):109–117.
- 510        32. Hessinger DA (1988) Nematocyst venoms and toxins. *The Biology of Nematocysts*  
511 (Elsevier), pp 333–368.
- 512        33. Pugh P (2001) A review of the genus erenna bedot, 1904 (siphonophora, physonectae).  
513 *BULLETIN-NATURAL HISTORY MUSEUM ZOOLOGY SERIES* 67(2):169–182.
- 514        34. Mitra A (2009) Are closure terms appropriate or necessary descriptors of zooplankton  
515 loss in nutrient–phytoplankton–zooplankton type models? *Ecological Modelling* 220(5):611–  
516 620.